


# Changes in Extreme Air Temperatures in One of South America's Longest Meteorological Records: Campinas, Brazil (1890-2022)

Lívia Braz Pereira<sup>1</sup> , Letícia Lopes Martins<sup>1</sup> , Iam Caio Abreu Rodrigues<sup>1</sup> , Graciela da Rocha Sobierajski<sup>2,\*</sup> , Gabriel Constantino Blain<sup>3</sup> 

1. Instituto Agrônomo  – Programa de Pós-graduação em Agricultura Tropical e Subtropical - Campinas (SP), Brazil.

2. Instituto Agrônomo  – Centro de Fruticultura – Jundiaí (SP), Brazil.

3. Instituto Agrônomo  – Centro de Biosistemas Agrícolas e Pós Colheira – Campinas (SP), Brazil.

**Received:** Jun. 7, 2023 | **Accepted:** Sep. 5, 2023

**Section Editor:** Patrícia Cia 

\***Corresponding author:** [graciela.rocha@sp.gov.br](mailto:graciela.rocha@sp.gov.br)

**How to cite:** Pereira, L. B., Martins, L. L., Rodrigues, I. C. A., Sobierajski, G. R. and Blain, G. C. (2023). Changes in Extreme Air Temperature in One of South America's Longest Meteorological Records: Campinas, Brazil (1890-2022). *Bragantia*, 82, e20230128. <https://doi.org/10.1590/1678-4499.20230128>

**ABSTRACT:** The frequency of extreme weather events has increased in almost all regions of the world. In this context, it is vital to understand how the location, scale, and shape of their frequency distributions are changing over time. This study used the flexibility of neural networks to model changes in the probability of daily extremes of maximum (Tmax) and minimum (Tmin) air temperature data in Campinas, Brazil — one of South America's longest meteorological records spanning from 1890 to 2022. Based on the Extremal Types Theorem, we employed a conditional density network to model the parameters of the generalized extreme value distribution (GEV-CDN) as functions of time. Our findings indicate that a GEV-based model, where the location and scale parameters vary over time, best described the variations in the Tmin series. However, a GEV-based model with only the location parameter varying over time best described the variations in the Tmax series. From an agrometeorological perspective, these results suggest that the probability of Tmax values leading to crop failures is rapidly increasing. The findings indicate a decrease in the probability of agronomic frost events in Campinas over the past 133 years, but the rate of this decrease has slowed in recent years. This result, combined with the negative value of the GEV's shape parameter, suggests that it is unlikely that Campinas may become an agronomic-frost-free region. To facilitate visualization of the changes in the probability of Tmax and Tmin values from 1890 to 2022, we have developed an internet application available at <https://climatology-iac.shinyapps.io/Shinny/>.

**Key words:** climate change, frost events, generalized extreme value distribution, weather extremes.

## INTRODUCTION

It is widely acknowledged that the frequency and intensity of extreme weather events have increased in almost all regions of the world (IPCC 2022), leading to unprecedented floods, heat waves, droughts, and frosts. In this regard, studies that have assessed trends in extreme air temperatures across the globe have observed changes consistent with increasing surface temperatures (Dunn et al. 2020; IPCC 2021). Additionally, changes in daily minimum temperatures are generally stronger than those observed in daily maximum temperatures (Dunn et al. 2020). In southeastern Brazil, authors such as Soares et al. (2016) and de Abreu et al. (2019) also detected trends toward warmer conditions. Climate change is often considered the primary cause of these increases, as it alters the frequency distribution of various climate variables and affects the likelihood of rare events occurring (IPCC 2021; Robin and Ribes 2020). Although the underlying mechanisms responsible for such changes are not fully understood, they are projected to continue into the future (IPCC 2022; Kharin et al. 2013), presenting an ongoing challenge to public safety, life, and the economy (Vörösmarty et al. 2013). In this context, one of

the primary challenges for studies that apply statistical methods to analyze extreme atmospheric events is to comprehend whether and how the location, scale, and shape of their frequency distributions are changing over time (Marengo et al. 2010).

Given the complexity of atmospheric dynamics, addressing this challenge requires highly flexible statistical models that can account for non-stationarities in model parameters (Coles 2001). From a climatological perspective, such non-stationary statistical models are expected to describe how the occurrence of extreme weather events is changing under current transient climate conditions in probabilistic terms (Blain et al. 2022). Although several probability functions can be used for this purpose, the generalized extreme value distribution (GEV) is the most common choice (Blain 2011; Coles 2001; Fontolan et al. 2019; Kharin et al. 2013, 2018; Litell et al. 2022; Robin and Ribes 2020; Xavier et al. 2019 a,b). The Extremal Types Theorem (ETT) often supports the use of the GEV distribution (Coles 2001; Wilks 2011). In addition, even when the assumptions of this theorem are not met, the GEV distribution is frequently a highly suitable choice (Wilks 2011).

Because of this widespread use and the significant impact of climate change on the probability of weather extremes, the GEV distribution has long been adapted to explicitly allow for non-stationarities in its parameters (Cannon 2010; Coles 2001; El Adlouni et al. 2007; Kharin and Zwiers 2004; Wang et al. 2004). In these studies, versions of the GEV were developed in which its parameters could be specified as functions of distinct covariates, such as time or other geophysical indices. However, the method proposed by Cannon (2010) is the only one that does not require *a priori* specification of the form of the relationship among the GEV parameters and their covariates. Specifically, the method proposed in the latter study models the relationship among the GEV parameters and covariates using a conditional density network (CDN), which is a probabilistic extension of the multilayer perceptron neural network. This method is referred to as GEV-CDN.

Due to its high flexibility, the GEV-CDN is capable of providing a deep understanding of how the location, scale, and shape parameters of the GEV are changing over time. This capability is particularly useful when the GEV-CDN is applied to long meteorological series, which allow placing the current extreme weather events in a historical regional perspective (MacDonald and Phillips 2006). Applying the GEV-CDN to these long-running meteorological series allows a detailed assessment on how climate change is affecting the frequency and intensity of extreme events that are rare by definition.

Regarding long-running air temperature series, the Agronomic Institute (IAC/APTA/SAA) has one of the oldest weather stations in South America, with daily records of maximum (T<sub>max</sub>) and minimum (T<sub>min</sub>) air temperatures dating back to 1890. This station is located at the institute's experimental farm in Campinas, State of São Paulo, Brazil and has virtually no missing data (further details are provided in the next section). Thus, this 133-year air temperature series presents an invaluable opportunity to test the hypothesis that the frequency and intensity of daily extremes for T<sub>max</sub> and T<sub>min</sub> in Campinas-SP are changing over time. Moreover, the use of highly flexible models to evaluate this hypothesis potentially allows for a detailed description of how the location, scale, and shape of the frequency distribution of T<sub>max</sub> and T<sub>min</sub> have changed over this 133-year period (1890-2022). Therefore, the aim of this study was to use the great flexibility of neural network architecture to model changes in the probability of daily extremes of T<sub>max</sub> and T<sub>min</sub> in Campinas-SP over the last 133 years under the framework of the non-stationary GEV distribution (GEV-CDN).

## DATA AND METHODS

### Data

Daily maximum and minimum air temperature data from the weather station of Campinas, State of São Paulo-Brazil (22°54'S; 47°05'W; 669m; 1890-2022) were used in this study. As previously described, the weather station (Fig. 1a) is situated at the Agronomic Institute's experimental farm. Since 1890, it has been relocated only once (Mello et al., 1994). The distance between its initial location (22°53'S; 47°05'W; 663m; 1890-1956) and its current location (22°54'S; 47°05'W; 669m; 1957-2022) is approximately 3 km, and these two meteorological series can be considered homogeneous (Mello et al. 1994). According to Conrad and Pollak (1950), two climate series are considered homogeneous when variations are caused only by changes in weather conditions. Mello et al. (1994) pointed out that these two series can be regarded as homogeneous. Because of this routine use, any missing records are replaced by data extracted manually from thermographs situated at the same site (Blain et al. 2018). The percentage of missing records is lower than 2%.

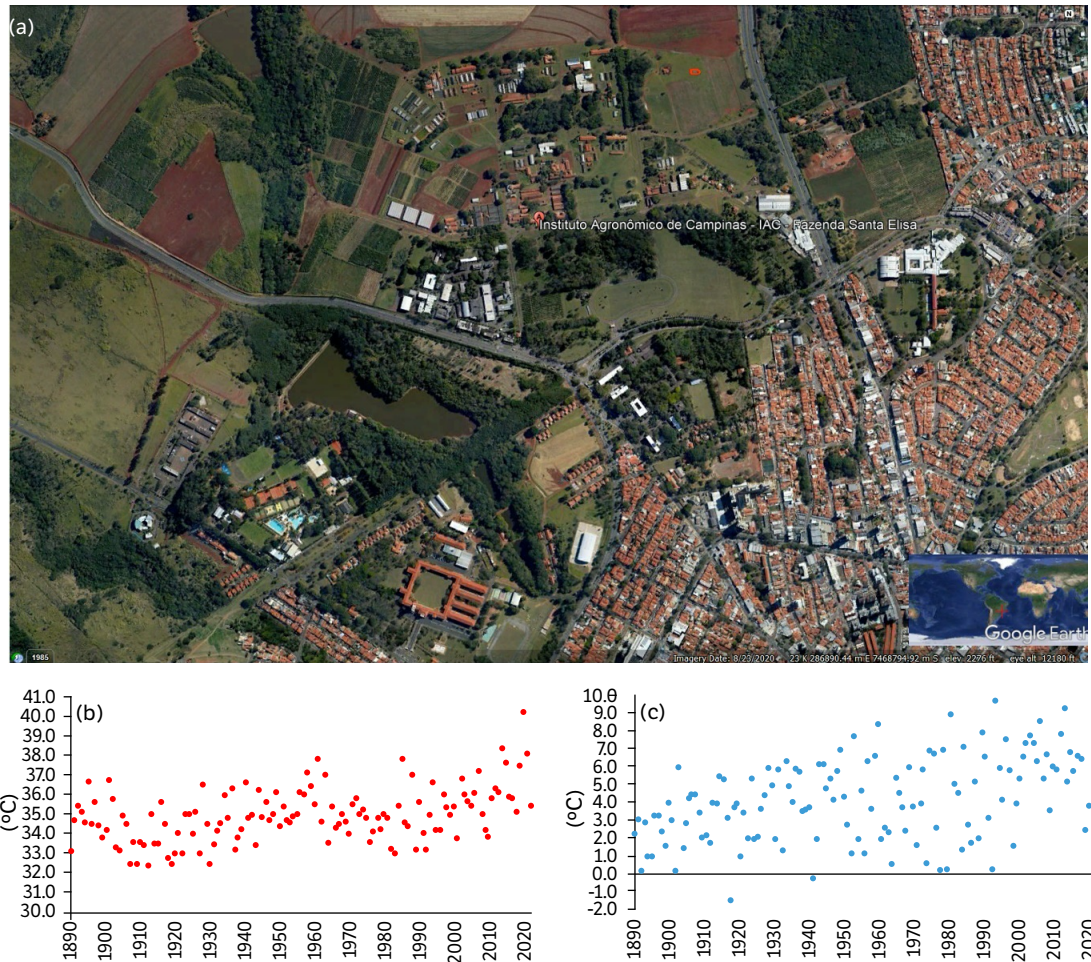


**Figure 1.** (a) Weather station of Campinas, State of São Paulo-Brazil (red dot); daily maximum (b) and minimum (c) air temperature data (block maxima approach).

Source: (a) Google Earth - <https://www.google.com.br/earth/>; (b) and (c) Elaborated by the authors.

As previously described, the *Extremal Types Theorem* postulates that the extremes of  $n$  independent data from a particular distribution approach the GEV probability function as  $n$  increases (Coles 2001; Wilks 2011). A typical example of extreme-value data is the collection of annual maximums, or block maximum in which the largest data observed within each year (block) is selected. This approach allows the application of the *Extremal Types Theorem*, since the time spans between two consecutive extreme-value data are often long. This results in a series with independent data. This approach can also be applied to collections of block minima (e.g.,  $T_{min}$  data), provided that a simple sign transformation  $T_{min} - T_{min}$  is applied (Coles 2001; Wilks 2011). The block maxima and minima series of Campinas are depicted in Fig. 1 b,c. We also made this data available at <[https://github.com/AgronomicInstitute/Weather\\_Campinas](https://github.com/AgronomicInstitute/Weather_Campinas)>.

## Methods

The entire range of possible limit distributions given by the Extremal Types Theorem are the Gumbel, Frechet and Weibull distributions. These three probability functions have distinct forms of tails decay, which lead to quite different representation of extreme value behaviors. The GEV's distribution (Eq. 1) combines these three functions into a single equation, in which the data themselves specifies the most appropriate type of tail decay (Gumbel, Frechet or Weibull) through the value of the shape parameter.

$$F(y; \mu, \alpha, k) = \exp \left[ - \left\{ 1 - k \frac{(y-\mu)}{\alpha} \right\}^{\frac{1}{k}} \right] \text{ for } k \neq 0, \text{ and } 1 - k \frac{(y-\mu)}{\alpha} > 0 \tag{1}$$

where  $\mu$ ,  $\alpha$ , and  $k$  are the location, scale and shape parameters.

The parameters of the GEV distribution are often estimated through the L-moments (Hosking 1990; Stedinger et al. 1993) or maximum likelihood method (ML). As described in the first section, the ML has been continually adapted to allow for nonstationarities in the GEV’s parameters (Cannon 2010; Coles 2001; El Adlouni et al. 2007; Kharin and Zwiers 2004; Wang et al. 2004). Despite this advantage over the L-moments, the ML method can lead to physically unrealistic values for the GEV’s shape parameter (Coles and Dixon 1999; Martins and Stedinger 2000). Martins and Stedinger (2000) overcame this difficulty by developing the generalized maximum likelihood estimation method (GML), which imposes a restrictive penalty on GEV’s shape parameter estimations. This penalty is based on the beta distribution (Eq. 2). As in Cannon (2010), we set  $c_1$  and  $c_2$  (Eq. 2) to 2 and 3.3, leading to a beta distribution with 90% of its probability mass concentrated between -0.4 and 0.2.

$$\pi_{(k)}^{(g)} = \text{Beta}(k + 0.5, c_1, c_2) \tag{2}$$

Considering that climate change alters the frequency distribution of various climatic variables and affects the probability of occurrence of rare events (Robin and Ribes 2020; IPCC 2021), the GEV distribution has been adapted to explicitly allow for no stationarities in its parameters (Cannon 2010; Coles 2001; El Adlouni et al. 2007; Kharin and Zwiers 2004; Wang et al. 2004). In this study, we performed such adaptation using the GEV-CDN to model the GEV’s parameters as functions of time. More specifically, we proposed 10 candidate models (Fig. 2) with increasing degrees of flexibility. The degree of flexibility of a GEV-CDN model can be specified by adjusting three aspects of the CDN.

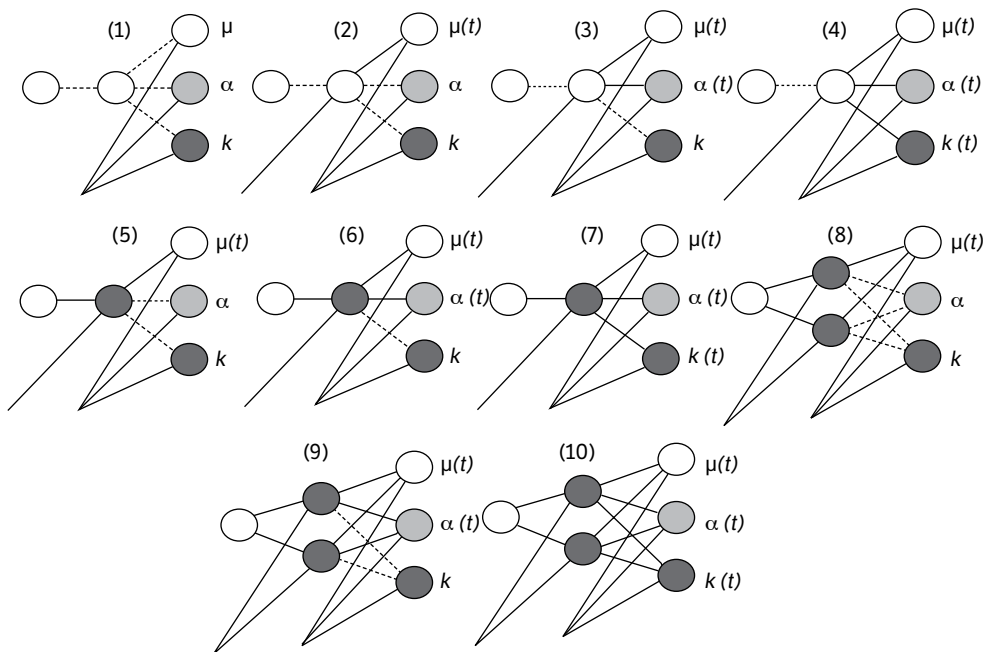


**Figure 2.** Neural network architectures of the 10 candidates GEV-based models (GEV-CDN) considered in this study ( $\mu$ ,  $\alpha$ , and  $k$  are the location, scale and shape parameters, respectively, of the GEV distribution and  $t$  is the time covariate).

Source: Elaborated by the authors.

(1) Choosing a hidden-layer activation function  $m(\cdot)$ ; Eqs. 3, 4 and 5). If  $m(\cdot)$  is chosen to be the hyperbolic tangent function  $\tanh(\cdot)$ , the relationship between the GEV parameter and its covariate is nonlinear. If  $m(\cdot)$  is chosen to be the identity function, the relationship between the GEV parameter and its covariate is linear.

(2) Connecting or disconnecting weights leading to output-layer nodes. Once a weight is disconnected, the parameter remains constant over time.

(3) Adjusting the number ( $J$ ) of hidden-layer nodes. Increasing the number of hidden-layer nodes increases the model's flexibility.

$$h_1(t) = m\left(\sum_{i=1}^I x_i(t)W_{ji}^{(1)} + b_j^{(1)}\right) \quad (3)$$

$$o_k(t) = \sum_{j=1}^J h_j(t)W_{kj}^{(2)} + b_k^{(2)} \quad (4)$$

$$\mu(t) = o_1(t) \quad (5.1)$$

$$\alpha(t) = \exp[o_2(t)] \quad (5.2)$$

$$k(t) = 0.5 \tanh[o_3(t)] \quad (5.3)$$

where  $W_{kj}^{(2)}$  and  $b_k^{(2)}$  represent the hidden-output layer weights and the hidden-output layer biases, respectively.

As described above, we fit 10 increasingly complex candidate models (Fig. 2) to the Tmax and Tmin series in order to evaluate a wide range of possible relationships between the GEV's parameters and the time and the GEV's parameters and the annual global air temperature. The simplest candidate model (model 1; Fig. 2) assumes that the GEV parameters do not vary over time. In other words, model 1 is the stationary GEV model with no covariate. Model 2 assumes that the network outputs  $o_1$  is a linear function of the covariate. Model 3 assumes that the network outputs  $o_1$  and  $o_2$  are linear functions of the covariate, model 4 assumes that the network outputs  $o_1$ ,  $o_2$ , and  $o_3$  are linear functions of the covariate. For models 2 to 4,  $m(\cdot)$  was taken to be the identity function. Models 5 to 7 have one hidden-layer node and are respectively similar to models 2 to 4, apart from the fact that  $m(\cdot)$  was taken to be the hyperbolic tangent function. Thus, models 5 to 7 allows for nonlinear relationships between the GEV parameters and their covariate. Models 8 to 10 are similar to models 5 to 7, apart from the fact that they have 2 hidden-layer nodes. In other words, they are highly flexible models able to describe a wide range of relationships between the GEV parameters and their covariate. As pointed out by Christiansen (2005), a neural network with two hidden-layer nodes can model a Z-shaped continuous curve. Therefore, we assumed that testing other candidate models with more than two hidden-layer nodes would increase the probability of overfitting and lead to no improvement in the understanding of how the GEV parameters are changing over time or as function of the global air temperature.

After fitting all the candidate models depicted in Fig. 2 to the Tmax and Tmin series of Campinas, the selection of "the most suitable model" for each of these variables becomes a key step for understanding how the location, scale, and shape of the GEV distributions have changed over the 133-year period (1890-2022). From an agrometeorological perspective, this selection process is expected to describe if and how the probability of the Tmax and Tmin events have changed over the last 133 years in Campinas-SP and if these changes are significantly correlated with the global air temperature. As pointed out by authors such as Cannon (2010); Coles (2001); El Adlouni et al. (2007) and Xavier et al. (2019a), this selection process should be based on the principle of parsimony, which seeks to choose the most parsimonious candidate model. In other words, this principle attempts to select the simplest model that explains as much of the variation in the data as possible (Coles 2001). More specifically, when the difference between two models is not evident it is preferable to use the simplest one (El Adlouni et al. 2007).

Several selection criteria are available in the literature. The Akaike information criterion (AIC), second-order Akaike information criterion (AICc; also known as corrected AIC for small sample sizes) and the Bayesian information criterion (BIC) are undoubtedly the most used (Cannon 2010; Coles 2001; Kharin et al. 2018; Strupczewski et al. 2001a,b; Sugahara et al. 2009; Villarini et al. 2009, 2010). In this study we adopted the AIC and AICc, because the BIC tends to select models that are too simple (i.e., underfitted) (Burnham and Anderson 2004) and may perform poorly when the dispersion of the series varies on time Xavier et al. (2019a) and Blain et al. (2022). The AIC and AICc selection criteria are derived from the Information-Theoretic approach (Burnham and Anderson 2004; Eqs. 6 and 7).

$$AIC = -2\log(ML) + 2c \quad (6)$$

Where  $\log(ML)$  is the maximized log likelihood function under the proposed model and  $c$  is the number of parameters in a given model. When the ratio between sample size ( $n$ ) and number of model's parameters ( $c$ ) is less than 40, the use of AICc instead of AIC has been suggested (Burnham and Anderson 2004; Fabozzi et al. 2014).

$$AICc = -2\log(ML) + 2c + \frac{2c(c+1)}{n-c-1} \quad (7)$$

As previously described, the candidate GEV-model that presents the lowest AIC and/or AICc value may be regarded as the best candidate model according to each of these selection criteria. The strength of evidence for each GEV-model depicted in Fig. 2 can also be evaluated by other two alternative methods: the  $\Delta AIC$  and the  $\Delta AICc$ . Although in principle the best model is the one that presents the lowest AIC or AICc value (Blain et al. 2022), other GEV-models with AIC or AICc values close to these lowest values may also be taken as suitable candidates (Blain et al. 2022; Burnham and Anderson 2004; Felici et al. 2007). In this context, the  $\Delta AIC$  or  $\Delta AICc$  of a candidate model is simply the difference between its AIC or AICc and the lowest AIC or AICc obtained among all models. As pointed out by Burnham and Anderson (2004), the models with  $\Delta AIC$  or  $\Delta AICc$  equal to or lower than 2 presents substantial evidence supporting its selection. Accordingly, in the cases in which two nested GEV-models presented  $\Delta AIC \leq 2$  or  $\Delta AICc \leq 2$ , we applied the likelihood ratio test (LRT; Eq. 5) to select the best model. The null hypothesis of the LRT assumes no difference between two nested models. Under this hypothesis, the LRT statistic is distributed according to a chi-square distribution with degrees-of-freedom equal to the difference between the number of each model's parameters. We performed the LRT test at the 5% significance level. In other words, LRT statistics (Eq. 8) with p-values equal to or lower than 0.05 led to the selection of the model with the higher number of parameters ( $M_j$ ); otherwise,  $M_i$  was selected.

$$LRT = \{\log(ML_j) - \log(ML_i)\} \text{ for } M_i \subset M_j \quad (8)$$

where  $\log(ML)$  is the maximized log likelihood function.

After selecting a candidate model for the Tmax and Tmin series, we applied the bagging predictors method (Breiman 1996) to estimate the values of each GEV-parameter. Specifically, while the AIC, AICc and LRT were used to define the number of hidden-layer nodes and which GEV-parameter are allowed to vary on time, the bagging predictors method was applied to fit an ensemble of the selected GEV-model using bootstrap aggregation (bagging). The number of ensembles GEV-models were set to 100. Because this ensemble is formed by constructing bootstrap replicates of the learning set which are then used as new learning sets (Breiman 1996), the bagging predictors method potentially improves accuracy of the GEV-parameter estimates.

We calculated confidence intervals for the GEV's parameters through a residual bootstrap-based method suggested by studies such as Khaliq et al. (2006). This procedure is described as follow. Step 1: we transformed the residuals ( $\varepsilon(t)$ ; Eq. 9) from the selected GEV-model into identically distributed data. Step 2: the data series formed by the  $\varepsilon(t)$  values were resampled with replacement leading to bootstrapped  $\varepsilon^*(t)$  series (this step was repeated 10000, resulting in 10000  $\varepsilon^*(t)$  series).

Step 3: we applied Eq. 10 to each  $\varepsilon^*(t)$  series to rescale the residuals [ $y^b(t)$ ]. Step 4: we fitted the selected GEV-model is fitted each  $y^*(t)$  sample. This resulted in a matrix with 1000 rows. The number of columns of this matrix is equal to the number of parameters of the selected GEV-model. Step 5. We calculated the 90% confidence interval for each parameter extracting the 5th and 95th percentiles of each column.

$$\varepsilon(t) = \left\{ 1 - k(t) \frac{[y(t) - \mu(t)]}{\alpha(t)} \right\}^{\frac{1}{k}} \quad (9)$$

$$y^b = \mu(t) - \alpha(t) \frac{\varepsilon^{(b)}(t) - 1}{k(t)} \quad (10)$$

Finally, we also developed an internet application <https://climatology-iac.shinyapps.io/Shinny/> that allows visualizing how the cumulative probabilities of several Tmax and Tmin values changed in Campinas from 1890 to 2022. This application was developed using the R Shiny package (Chang et al. 2023).

## RESULTS AND DISCUSSION

Before evaluating the results found in this study, it has to be emphasized that the nonstationary approach presented in section Methods is also a powerful parametric trend test (Blain 2011; 2022; Delgado et al. 2010; Kharin et al. 2013; Pujol et al. 2007; Sugahara et al. 2009; Xavier et al. 2019a). Different from nonparametric methods, such as the Mann-Kendall trend test (Kendall & Stuart 1967; Mann 1945), the nonstationary approach applied in this study is able to detect and describe changes in the probabilistic structure of the Tmax and Tmin series (Blain et al. 2022). More specifically, consider the 10 increasingly complex candidate models proposed in this study. If the stationary model (model 1: a GEV model with parameters constant over time) is selected as the one that best explains the variation in the data, we should conclude that there is no evident sign of climate change in this 133-year data sample (Pujol et al. 2007). Otherwise, if a nonstationary model is selected (models 2 to 10: GEV models with time-varying parameter) we may conclude that there are signs of climate change in the data sample. As described in the next sections, when the covariate was time, the best GEV-models for Tmax (model 2) and Tmin (model 9) are nonstationary functions in which the location (Tmax) and both location and scale parameters (Tmin) vary as function of time. Considering the wide range of candidate models proposed in this study, this nonstationary approach also enabled a broad understanding of the trend isolating its effect on the location (central tendency), scale (dispersion) and shape (tail behavior) of the air temperature frequency-distributions. These results are presented below.

### Selecting the best GEV-models

Regarding the minimum air temperature, the AICc and  $\Delta$ AICc indicated that models 9 and 3 (Table 1, in blue) can be used to explain the variation in the Tmin in Campinas-SP over the last 133 years (1890-2022). The AIC and  $\Delta$ AIC ranked models 3, 9 and 6 as the best, second-best and third-best candidates for this Tmin series (Table 1, in blue). These results, derived from the AIC and AICc, are consistent with each other since these three nested models allow the GEV-location and GEV-scale parameters to vary on time (Cannon, 2010). The disagreement among these 3 models is related to the form (linear or nonlinear) of these changes.

Considering the results of Table 1, we applied the LRT test to select among models 3, 6 and 9 as follow: models 3 and 6 are those with the lower number of parameters, therefore we first applied the LRT to select between these two candidates. The  $\log(ML)$  of each model is 40.74 and 41.99, respectively, and the difference between the number of parameters is 2. The p-value of the resulting LRT statistic was 0.29, what indicated that the higher complexity of candidate 6 led to no significant

improvement in respect to candidate 3. Thus, we initially selected model 3. The LRT test was applied again to select from models 9 and 3. The  $\log(ML)$  of model 9 is 47.42 and the difference between the number of parameters is 6. The p-value of the LRT statistic was lower than the adopted significant level (p-value=0.037). As an extra verification, we applied the LRT test to models 9 and 6. The resulting p-value was 0.027. Therefore, we select model 9 as the candidate that best explains the variation in the  $T_{min}$  in Campinas-SP (1890 to 2022) as a function of time. Accordingly, we may conclude that the central tendency and the dispersion of the  $T_{min}$  series has increased in a nonlinear way since 1890 (Blain 2011; Cannon 2010; Coles 2001; El Adlouni et al. 2007; Wilks 2011).

**Table 1.** Second-order Akaike information criterion (AICc), Akaike information criterion (AIC), and their corresponding delta method ( $\Delta AICc$  and  $\Delta AIC$ ) applied to nonstationary GEV-based models fitted to daily extremes for the minimum air temperature in Campinas (SP), Brazil (1890-2022).

Candidate	AICc	AIC	$\Delta AICc$	$\Delta AIC$
model 1	-40.81	-41.00	31.90	30.19
model 2	-67.89	-68.21	4.69	3.10
model 3	-71.00	-71.47	1.43*	0.00*
model 4	-68.82	-69.49	3.41	2.17
model 5	-63.66	-64.33	8.57	7.33
model 6	-69.03	-69.93	2.97	1.96*
model 7	-66.76	-67.92	4.98	4.24
model 8	-64.96	-66.42	6.48	6.04
model 9	-70.72	-72.90	0.00*	0.28*
model 10	-67.75	-70.80	2.09	3.25

\* Suitable models, according to each method. Source: Elaborated by the authors.

Regarding the maximum air temperature, the AIC, AICc,  $\Delta AIC$ , and  $\Delta AICc$  criteria selected model 8 as the best candidate to explain the variation in the  $T_{max}$  in Campinas-SP as function of time (Table 2, in blue). Model 8 is a nonstationary function in which only the GEV-location parameter varies on time. Since the hidden-layer activation function of this model is the hyperbolic tangent function, we may conclude that the central tendency of this  $T_{max}$  series has increased in a nonlinear way since 1890 (Blain 2011; Cannon 2010; Coles 2001; El Adlouni et al. 2007; Wilks 2011).

**Table 2.** Second-order Akaike information criterion (AICc), Akaike information criterion (AIC), and their corresponding delta method ( $\Delta AICc$  and  $\Delta AIC$ ) applied to nonstationary GEV-based models fitted to daily extremes for the maximum air temperature in Campinas-SP, Brazil (1890-2022).

Candidate	AICc	AIC	$\Delta AICc$	$\Delta AIC$
model 1	-86.08	-86.27	34.45	33.17
model 2	-109.05	-109.37	11.35	10.20
model 3	-107.80	-108.28	12.44	11.45
model 4	-106.35	-107.02	13.70	12.90
model 5	-109.30	-109.96	10.76	9.96
model 6	-107.83	-108.73	11.99	11.42
model 7	-106.26	-107.42	13.29	12.99
model 8	-119.25	-120.72	0.00*	0.00*
model 9	-115.27	-117.45	3.27	3.98
model 10	-110.85	-113.90	6.81	8.41

\* Suitable models, according to each method.

Figure 3 depicts the temporal changes in the GEV-parameters for  $T_{min}$  and  $T_{max}$  series in Campinas-SP from 1890 to 2022. As previously described, the parameters estimates were calculated through the bagging predictors method, considering



a GEV-based model with two hidden-layer nodes in which both location and scale parameters are allowed to vary on time (for Tmin) and another GEV-based model with two hidden-layer nodes in which only the location parameter is allowed to vary on time.

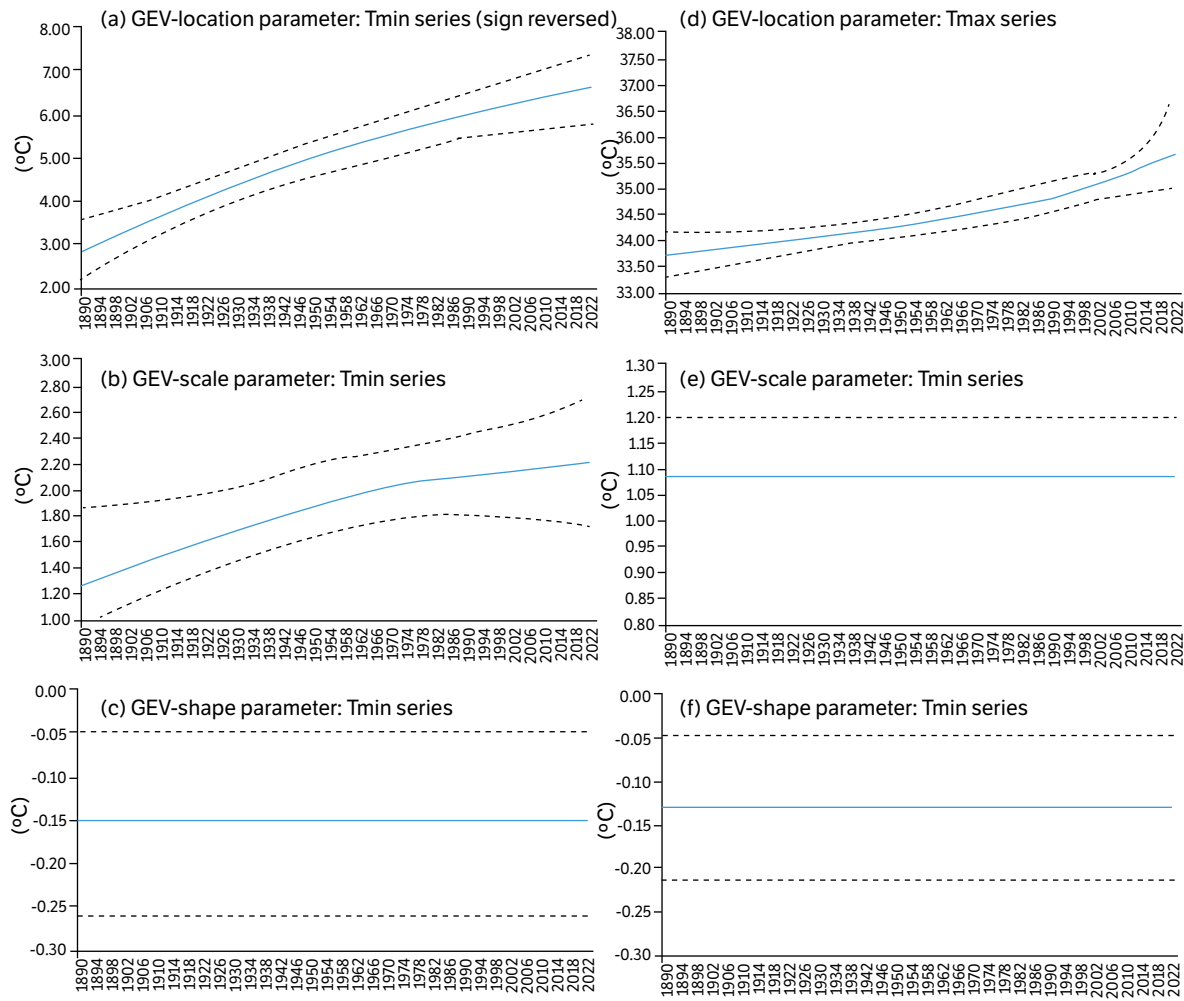


**Figure 3.** Location, Scale and Shape parameters of two nonstationary GEV-based models fitted to daily extremes for the minimum (a to c) and maximum (d to f) air temperature series in Campinas-SP, Brazil (1890-2022). The dotted lines are the confidence intervals.

Source: Elaborated by the authors.

The results depicted in Tables 1 and 2 and Fig. 3 indicates significant signs of long-term trends in both Tmax and Tmin series of Campinas (1890-2022) with different temporal patterns in trends of these two series. Although both series presented trends to warmer conditions – described by the increasing values of the GEV-location parameters – the Tmin series showed a GEV-scale parameter that also increased over the last 133 years. In other words, while only the central tendency of the Tmax data increased over time, both the central tendency and dispersion of the Tmin data increased between 1890 and 2022. From a meteorological perspective, this suggests that distinct responses to forcing mechanisms or feedback processes, such as urbanization, land use changes, cloud feedback, and increases in atmospheric concentrations of greenhouse gases, must be present to produce these different behaviors (Cordeiro et al. 2011). Despite these different signatures regarding the scale GEV-parameter, none of the models found suitable by the selection criteria (Tables 1 and 2) have a time-varying GEV-shape parameter. This result concurs with the statement that the latter GEV-parameter is unlikely to be affected by climate change (although the scale may) as it is invariant temporally with latitude (Wilson and Toumi 2005). In addition,

the negative values of the GEV-shape parameters depicted in Fig. 3 describe probability density functions that decreases slowly for large (low) values of  $T_{max}$  ( $T_{min}$ ) (Wilks 2011).

From an agrometeorological perspective, the GEV-parameters depicted in Fig. 3 indicates that the probability of occurring high  $T_{max}$  values that may lead to crop failures increased over the last 133 years in Campinas. Regarding the  $T_{min}$  series, although the increasing trend in the location parameter would decrease the probability of agronomic frost events, the increasing values of the GEV-scale parameter and the negative value of the GEV-shape parameter prevent the conclusion that the probability of the latter agrometeorological hazard in Campinas-SP may approach zero (Blain 2011). In simple terms, despite the significant changes to warmer conditions observed in this location, the increasing trends in the dispersion of the daily extreme for the minimum air temperature, along with the heavy tail of its frequency distribution (negative GEV-shape parameter), do not allow us to state that Campinas is becoming a frost-free region. This issue is further evaluated in the next section.

### Agrometeorological perspective: Practical implications

Before evaluating the possible agrometeorological impacts of the trends found in the  $T_{max}$  and  $T_{min}$  series, we must define frost events from the agronomic viewpoint. Frost is an atmospheric hazard that causes damage to plants due to their exposure to low temperatures that fall below their resistance to freezing (Pereira et al. 2002). Thus, it depends on the weather conditions, the cultivar, and its phenological phase. In the State of São Paulo, the minimum air temperature is the main element that triggers this event, which may occur with or without ice formation (white and black frosts, respectively; Pereira et al. 2002). As pointed out by Braga et al. (2021) when the air temperature value (measured at the meteorological shelter; Sentelhas et al. 1995) falls below 4°C species such as banana, potato, beans, greenery, papaya and tomato may face agronomical frost. When the air temperature values falls below 2°C species such as coffee, soybeans, sugar cane, mango and wheat may also face this agronomical hazard. Because of the increasing values of the GEV-location parameter, the cumulative probability of such critical air temperature values (e.g., 4°C and 2°C) decreased over the last 133 years in Campinas-SP (Fig. 4). However, the increasing values of the GEV-scale and the negative value of the GEV-shape parameters has limited such decay. In other words, the slope of curves depicted in Fig. 4 has decreased over time. Regarding the  $T_{max}$  series, air temperatures values above 34°C and 35°C during flowering may put negative pressure on coffee and citrus yields, respectively. (e.g., Davies and Albrigo 1994; Monteiro 2009). Figure 4 depicts how the cumulative probability of such critical thresholds' changes in Campinas-SP, over the last 133 year.

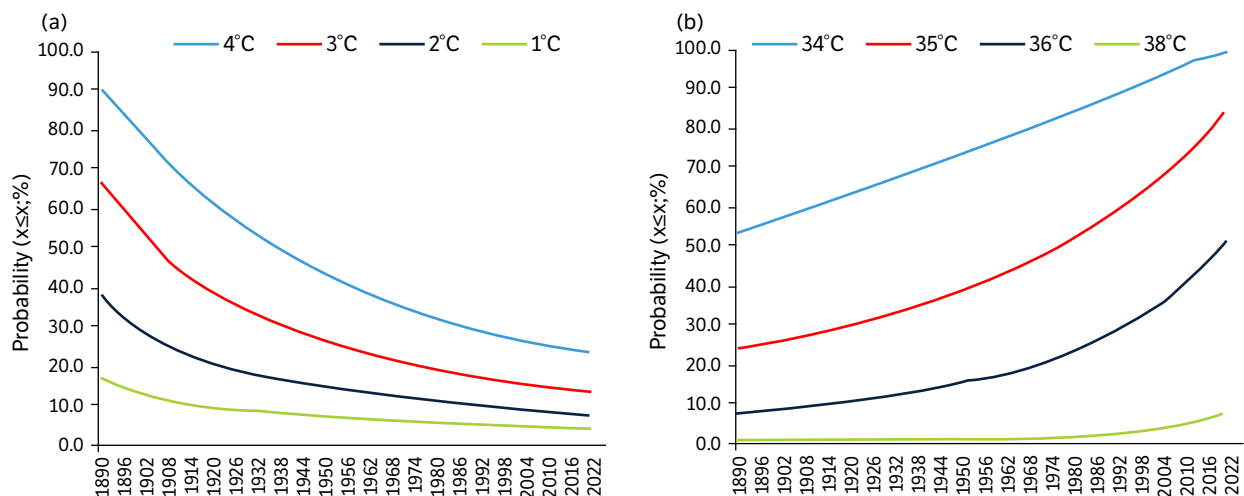


**Figure 4.** Cumulative probability  $[\Pr(x \leq X)]$  of minimum (a) and maximum (b) air temperature values as a function of time. Campinas, state of São Paulo, Brazil (1890-2022).

Source: Elaborated by the authors.

The results depicted in Fig. 4 exemplify the significant effects that climate change may have on the probability of extreme agrometeorological events. Regarding the minimum air temperature series (Fig. 4a), the probability of having at least one day in a year with  $T_{min} \leq 4^{\circ}\text{C}$  varied from ~85%, during the last decade of the XIX century, to ~24%, during 2013-2022. For  $T_{min}$  values equal to or lower than  $2^{\circ}\text{C}$  this probability decreased from ~34% to 8%, considering the same periods. Despite this remarkable change to warmer conditions, Fig. 4a also described that the slope of these trends decreased as the cumulative probabilities of these events moved toward the tail of the distribution (became more extreme in probabilistic terms). As previously described, this behavior is explained by the negative value of the GEV-shape parameter and the increasing values of the GEV-scale parameter (Fig. 3b,c). In other words, although the probabilistic modelling of the  $T_{min}$  series of Campinas has described a remarkable change to warmer conditions, it does not allow us to state that this region may become free from agronomic frost events due to the current global warming.

The  $T_{max}$  series also presented remarkable changes to warmer conditions between 1890 and 2022. For instance, the probability of having at least one day in a year with  $T_{max} \geq 34^{\circ}\text{C}$  varied from ~54%, during the last decade of the XIX century, to ~97%, during 2013-2022. For  $T_{max}$  values equal to or larger than  $36^{\circ}\text{C}$  this probability increased from ~9% to 47%, considering the same periods. However, opposite to what was observed for the  $T_{min}$  series, the slope of these trends increased over the time. Although the GEV-shape parameter is also negative (Fig. 3f), the GEV-scale parameter did not change on time (Fig. 3e) and the GEV-location parameter presented a nonlinear trend with a slope that increased over the last years (Fig. 3d).

## CONCLUSION

Taking advantage of the great flexibility of the GEV-CDN (Cannon, 2010), we performed a detailed description of how the location, scale, and shape of the frequency distributions of daily extremes for maximum ( $T_{max}$ ) and minimum ( $T_{min}$ ) air temperature data changed over the last 133 years (1890-2022) in Campinas, state of São Paulo, Brazil. Among 10 candidate models, we found that nonstationary and nonlinear GEV models are those that best explain the variation in both  $T_{max}$  and  $T_{min}$  series. Specifically, for the  $T_{min}$  series, the best candidate was a GEV-based model in which the location and scale parameters vary on time. For the  $T_{max}$  series, the best candidate was a GEV-based model in which only the location parameter varies on time. Although both series presented trends to warmer conditions, these different signatures regarding the scale parameter suggest that different forcing mechanisms or feedback processes must be present to produce these different responses (Cordeiro et al. 2011). In other words, while the warming in the  $T_{max}$  data has intensified over the last 22 years (~2000 to 2022), the slope of the trends found in the probability of  $T_{min}$  values has decreased in the same period. From an agrometeorological perspective, these results indicated that the probability of occurring  $T_{max}$  values, which may lead to crop failures, are fast increasing. These results also indicated that the probability of occurring agronomic frost events in Campinas decreased over the last 133 years (from ~ 85%, during the last decade of the XIX century, to ~24%, during 2013-2022). However, the rate of these changes to warmer conditions has also decreased in recent years. This result along with the negative value of the shape parameter suggest that it is very unlikely that Campinas may become an agronomic frost-free region due to global warming. We also developed an internet application <<https://climatology-iac.shinyapps.io/Shinny/>> that allows visualizing the temporal changes in the probability of  $T_{max}$  and  $T_{min}$  from 1890 to 2022.

## AUTHORS' CONTRIBUTION

**Conceptualization:** Martins, L. L., Sobierajski, G. R. and Blain, G. C.; **Investigation:** Martins, L. L., Pereira, L. B., Rodrigues, I. C. A., Sobierajski, G. R. and Blain, G. C.; **Methodology:** Martins, L. L., Sobierajski, G. R. and Blain, G. C.; **Formal analysis:** Sobierajski, G. R. and Blain, G. C.; **Data acquisition:** Blain, G. C.; Software: Blain, G. C.; **Validation:** Martins, L. L., Rodrigues, I. C. A. and Blain, G. C.; **Writing – original draft:** Martins, L. L., Sobierajski, G. R. and Blain,

G. C.; **Writing – review & editing:** Martins, L. L., Rodrigues, I. C. A., Pereira, L. B., Sobierajski, G. R. and Blain, G. C.; **Visualization:** Blain, G. C.; **Supervision:** Blain, G. C.

## DATA AVAILABILITY STATEMENT

The data used in this study is available at <[https://github.com/AgronomicInstitute/Weather\\_Campinas](https://github.com/AgronomicInstitute/Weather_Campinas)>.

## FUNDING

Conselho Nacional de Desenvolvimento Científico e Tecnológico

<https://doi.org/10.13039/501100003593>

Grant No: 304609/2022-6

Coordenação de Aperfeiçoamento de Pessoal de Nível Superior

<https://doi.org/10.13039/501100002322>

Finace code 001

## ACKNOWLEDGMENTS

To National Council for Scientific and Technological Development (CNPq Process 304609/2022-6) for provide the grant for the fifth author. This study was financed in part by the Coordenação de Aperfeiçoamento de Pessoal de Nível Superior – Brasil (CAPES) – Finace Code 001.

## REFERENCES

- Abreu R., Tett, S., Schurer A. and Rocha H. (2019). Attribution of Detected Temperature Trends in Southeast Brazil. *Geophysical Research Letters*, 46, 8407-8414. <https://doi.org/10.1029/2019GL083003>
- Blain G. C., Picoli M. C. A. and Lulu J. (2009). Análises estatísticas das tendências de elevação nas séries anuais de temperatura mínima do ar no Estado de São Paulo. *Bragantia*, 68, 807-815. <https://doi.org/10.1590/S0006-87052009000300030>
- Blain, G. C. (2011). Incorporating climate trends in the stochastic modeling of extreme minimum temperature series of Campinas, state of São Paulo, Brazil. *Bragantia*, 70, 952-957. <https://doi.org/10.1590/S0006-87052011000400031>
- Blain, G.C., De Avila, A.M.H. and Pereira, V.R. (2018) Using the normality assumption to calculate probability based standardized drought indices: selection criteria with emphases on typical events. *International Journal of Climatology*, 38, e418–e436. <https://doi.org/10.1002/joc.5381>
- Blain, G. C., Sobierajski, G. R., Weight, E., Martins, L. L. and Xavier, A. C. F. (2022). Improving the interpretation of standardized precipitation index estimates to capture drought characteristics in changing climate conditions. *International Journal of Climatology*, 45, 11, 5586-5608. <https://doi.org/10.1002/joc.7550>
- Braga, G. B., Imbuzeiro, H. M. A., Pires, G. F., Oliveira, L. R., Barbosa, R. A. and Vilela, K. F. (2021). Frost Risk and Rural Insurance in Brazil. *Revista Brasileira de Meteorologia*, 36, 703-711. <https://doi.org/10.1590/0102-7786360137>
- Breiman, L. (1996). Bagging predictors. *Machine learning*, 24, 123–140.

- Burnham, K. P. and Anderson, D. R. (2004). Multimodel inference: understanding AIC and BIC in model selection. *Sociological Methods & Research*, 33, 261-304. <https://doi.org/10.1177/0049124104268644>
- Cannon, A. J. (2010). A flexible nonlinear modelling framework for nonstationary generalized extreme value analysis in hydroclimatology. *Hydrological Process*, 24, 673-685. <https://doi.org/10.1002/hyp.7506>
- Chang, W., Cheng, J., Allaire, J., Sievert, C., Schloerke, B., Xie, Y., Allen, J., McPherson, J., Dipert, A. and Borges B. (2023). shiny: Web Application Framework for R. R package version 1.7.4.9002, <https://shiny.rstudio.com/>.
- Christiansen, B. (2005). The short comings of nonlinear principal component analysis in identifying circulation regimes. *Journal of Climate*, 18, 4814-4823. <https://doi.org/10.1175/JCLI3569.1>
- Coles, S. G. and Dixon, M. J. (1999). Likelihood-based inference for extreme value models. *Extremes* 2, 5-23. <https://doi.org/10.1023/A:1009905222644>
- Coles, S. (2001). *An Introduction to Statistical Modeling of Extreme Values*. Springer: London.
- Conrad, V. and C. Pollak. (1950). *Methods in Climatology*. 2d ed. London: Harvard University Press.
- Cordeiro, E. C., Kessomkiat, W., Abatzoglou, J. and Mauget, S. (2011). The identification of distinct patterns in California temperature trends. *Climatic Change*, 108, 357-382. <https://doi.org/10.1007/s10584-011-0023-y>
- Davies, F. S. and Albrigo L. G. (1994). *Citrus*. Wallingford: CAB International, Wallingford.
- Delgado, J. M., Apel, H. and Merz, B. (2010). Flood trends and variability in the Mekong river. *Hydrology and Earth System Sciences*, 14, 407-418. <https://doi.org/10.5194/hess-14-407-2010>
- Dunn, R. J. H., Alexander, L. V., Donat, M. G., Zhang, X., Bador, M., Herold, N., Lippman, T., Allan, R., Aguilar, E., Barry, A. A., Brunet, M., Caesar, J., Chagnaud, G., Cheng, V., Cinco, T., Durre, I., Guzman, R., Htay, T. M., Ibadullah, W. M. W., Ibrahin, I. B., Khoshkam, M., Kruger, A., Kubuta, H., Leng, T. W., Lim, g., Li-Sha, L., ?Marengo, J., Mbatha, S., McGree, S., Menne, M., Skansi, M. M., Ngwenya, S., Nkrumah, F., Oonariya, C., Pabon-Caicedo, J. D. P., Panthou, G., Pha, C., Rahimzadeh, F., Ramos, A., Salgado, E., Salinger, J., Sané, Y., Sopaheluwakan, A., Srivastava, A., Sun, Y., Timbal, B., Trachow, N., Trewin, B., van der Schrier, G., Vazquez-Aguirre, J., Vasquez, R., Villarroel, C., Vincent, L., Vischel, T., Vose, R. and Yussof, M. N. B. H. (2020). Development of na Updated Global Land In Situ-Based Data Set of Temperature and Precipitation Extremes: HadEX3. *Journal of Geophysical Research: Atmospheres*, 125, 16. <https://doi.org/10.1029/2019JD032263>
- El Adlouni, S., Ouarda, T. B. M. J., Zhang, X., Roy, R. and Bobée, B. (2007). Generalized maximum likelihood estimators for the nonstationary generalized extreme value model. *Water Resources Research*, 43, W03410. <https://doi.org/10.1029/2005WR004545>
- Fabozzi, F. J., Focardi, S. M., Rachev, S. T. and Arshanapalli, B. G. (2014). Appendix E: Model Selection Criterion: AIC and BIC. *The Basics of Financial Econometrics: Tools, concepts, and Asset Management Applications*. New York: John Wiley. <https://doi.org/10.1002/9781118856406.app5>
- Felici, M., Lucarini, V., Speranza, A. and Vitolo, R. (2007). Extreme value statistics of the total energy in an intermediate-complexity model of the midlatitude atmospheric jet. Part II: trend detection and assessment. *Journal of the Atmospheric Sciences*, 64, 2159-2175. <https://doi.org/10.1175/JAS4043.1>
- Fontolan, M., Xavier, A. C. F., Pereira, H. R. and Blain, G. C. (2019). Using climate models to assess the probability of weather extremes events: a local scale study based on the generalized extreme value distribution. *Bragantia*, 78, 146-157. <https://doi.org/10.1590/1678-4499.2018144>
- Hosking, J.R.M. (1990). L-moments: analysis and estimation of distributions using linear combinations of order statistics. *Journal of the Royal Statistical Society*, B52, 105-124. <https://doi.org/10.1111/j.2517-6161.1990.tb01775.x>
- [IPCC] Intergovernmental Panel on Climate Change. (2021). Summary for Policymakers. In Masson-Delmotte, V., P. Zhai, A. Pirani, S.L. Connors, C. Péan, S. Berger, N. Caud, Y. Chen, L. Goldfarb, M.I. Gomis, M. Huang, K. Leitzell, E. Lonnoy, J.B.R. Matthews, T.K. Maycock, T. Waterfield, O. Yelekçi, R. Yu, and B. Zhou (Eds.), *Climate Change 2021: The Physical Science Basis. Contribution of Working Group I*

to the Sixth Assessment Report of the Intergovernmental Panel on Climate Change. (p. 3–32). Cambridge: Cambridge University Press. <http://doi.org/10.1017/9781009157896.001>

[IPCC] Intergovernmental Panel on Climate Change. (2022). Climate Change 2022: Impacts, Adaptation, and Vulnerability. Contribution of Working Group II to the Sixth Assessment Report of the Intergovernmental Panel on Climate Change. In H.-O. Pörtner, D.C. Roberts, M. Tignor, E.S. Poloczanska, K. Mintenbeck, A. Alegría, M. Craig, S. Langsdorf, S. Lösschke, V. Möller, A. Okem and B. Rama (Eds.). Cambridge: Cambridge University Press. <https://doi.org/10.1017/9781009325844>

Kendall, M. A. and Stuart, A. (1967). The advanced theory of statistics 2nd ed. Londres: Charles Griffin.

Khaliq, M.N. and Ouarda, T.B.M.J. (2007). On the critical values of the standard normal homogeneity test (SNHT). *International Journal of Climatology*, 27, 681–687. <https://doi.org/10.1002/joc.1438>

Kharin, V.V. and Zwiers, F.W. (2004). Estimating extremes in transient climate change simulations. *Journal of Climate*, 18, 1156–1173. <https://doi.org/10.1175/JCLI3320.1>

Kharin, V. V., Zwiers, F. W., Zhang, X. and Wehner, M. (2013). Changes in temperature and precipitation extremes in the CMIP5 ensemble. *Climatic Change*, 119, 345-357. <https://doi.org/10.1007/s10584-013-0705-8>

Kharin, V. V., Flato, G. M., Zhang, X., Gillett, N. P., Zwiers, F. and Anderson, K. J. (2018). Risks from Climate Change Differently from 1.5 °C to 2.0 °C Depending on Rarity. *Earth's Future*, 6, 704-715. <https://doi.org/10.1002/2018EF000813>

Litell, M. F., Xavier, A. C. F. and Blain, G. C. (2022). Evaluation of nested climate change models in the study of extreme events. *Journal of Earth System Science*, 131, 120. <https://doi.org/10.1007/s12040-022-01853-w>

MacDonald, N. and Phillips, I. D. (2006). Reconstructed annual precipitation series for Scotland (1861-1991): Spatial and temporal variations, and links to the atmospheric circulation. *Scottish Geographical Journal*, 122, 1-18. <https://doi.org/10.1080/00369220600830771>

Mann, H.B. (1945). Non-parametric tests against trend. *Econometrica*, 13, 245-259.

Marengo, J. Rusticucci, M., Penalba, O. and Renom, M. (2010). Na intercomparison of observed and simulated extreme rainfall and temperature events during the last half of the twentieth century: par 2: historical trends. *Climatic Change*, 98, 509-529. <https://doi.org/10.1007/s10584-009-9743-7>

Martins, E. S. and Stedinger, J. R. (2000). Generalized maximum likelihood generalized extreme-value quantile estimators for hydrologic data. *Water Resources Research*, 36, 737-744. <https://doi.org/10.1029/1999WR900330>

Mello, M.H.A., Pedro Júnior, M.J., Ortolani, A.A. and Alfonsi, R.R. (1994). Chuva e temperatura: cem anos de observações em Campinas. Campinas: Instituto Agronômico.

Monteiro, J. E. B. A. (2009). Agrometeorologia dos cultivos: o fator meteorológico na produção. Brasília, DF: INMET.

Pereira, A. R., Angelocci, L. R. and Sentelhas, P.C. (2002). Agrometeorologia: fundamentos e aplicações práticas. Guaíba: Agropecuária.

Pujol, N., Neppel, L. and Sabatier, R. (2007). Regional tests for trend detection in maximum precipitation series in the French Mediterranean region. *Hydrological Sciences Journal*, 52, 956–973. <https://doi.org/10.1623/hysj.52.5.956>

Robin, Y. and Ribes, A. (2020). Nonstationary extreme value analysis for even attribution combining climate models and observations. *Advances in Statistical Climatology, Meteorology and Oceanography*, 6, 205-221. <https://doi.org/10.5194/ascmo-6-205-2020>

Sentelhas, P.C., Piza Junior, C.T., Alfonsi, R. R., Kavati, R. and Soares, N.B. (1995). Zoneamento climático da época de maturação do abacate no estado de São Paulo. *Revista Brasileira de Agrometeorologia*, 3, 133-140. <https://www.sbagro.org/files/biblioteca/70.pdf>

Soares, D. B., Lee, H., Loikith, P., Barkhordarian, A. and Mechoso, C. R. (2016). Can significant trends be detected in surface air temperature and precipitation over South America in recent decades?. *International Journal of Climatology*, 37, 1483-1793. <https://doi.org/10.1002/joc.4792>

- Stedinger, J.R., Vogel, R.M. and Foufoula-Georgiou, E. (1993). Frequency analysis of extreme events. In D.R. Maidment (Ed.), *Handbook of Hydrology*. (p. 1-18). New York: McGraw-Hill.
- Strupczewski, W. G., Singh, V. P. and Feluch, W. (2001a). Nonstationary approach to at-site flood frequency modelling I. Maximum likelihood estimation. *Journal of Hydrology*, 248, 123-142. [https://doi.org/10.1016/S0022-1694\(01\)00397-3](https://doi.org/10.1016/S0022-1694(01)00397-3)
- Strupczewski, W. G., Singh, V. P. and Mitosek, H. T. (2001b). Nonstationary approach to at-site flood frequency modelling. III. Flood analysis of Polish rivers. *Journal of Hydrology*, 248, 152-167. [https://doi.org/10.1016/S0022-1694\(01\)00399-7](https://doi.org/10.1016/S0022-1694(01)00399-7)
- Sugahara, S., da Rocha, R. P. and Silveira, R. (2009). Non stationary frequency analysis of extreme daily rainfall in Sao Paulo, Brazil. *International Journal of Climatology*, 29, 1339-1349. <https://doi.org/10.1002/joc.1760>
- Villarini, G., Serinaldi, F., Smith, J. A. and Krajewski, W. F. (2009). On the stationarity of annual flood peaks in the continental United States during the 20th century. *Water Resources Research*, 45, 1-17. <https://doi.org/10.1029/2008WR007645>
- Villarini, G., Smith, J. A. and Napolitano, F. (2010). Nonstationary modeling of a long record of rainfall and temperature over Rome. *Advances in Water Resources*, 33, 1256-1267. <https://doi.org/10.1016/j.advwatres.2010.03.013>
- Vörösmarty, J. C., Guenni, L. B., Wollheim, W. M., Pellerin, B., Bjerklie, D., Cardoso, M., D'Almeida, C., Green, P. and Colon, L. (2013). Extreme rainfall, vulnerability and risk: a continental-scale assessment for South America. *Philosophical Transactions of the Royal Society a Mathematical, Physical and Engineering Sciences*, 371, 20120408. <https://doi.org/10.1098/rsta.2012.0408>
- Wang, X. L., Zwiers, F. W. and Swail, V. R. (2004). North Atlantic Ocean wave climate change scenarios for the twenty-first century. *Journal of Climate*, 17, 2368–2383. [https://doi.org/10.1175/1520-0442\(2004\)017<2368:NAOWCC>2.0.CO;2](https://doi.org/10.1175/1520-0442(2004)017<2368:NAOWCC>2.0.CO;2)
- Wilks, D. S. (2011). *Statistical Methods in the Atmospheric Sciences*. San Diego, CA: Academic Press, 100, 704.
- Wilson, P. S. and Toumi, R. (2005). A fundamental probability distribution for heavy rainfall. *Geophysical Research Letters*, 32, 14. <https://doi.org/10.1029/2005GL022465>
- Xavier, A. C. F., Blain, G. C., Morais, M. V. B., Sobierajski, G. R. (2019a). Selecting “the best” nonstationary Generalized Extreme Value (GEV) Distribution: on the influence of different numbers of GEV-models. *Bragantia*, 78, 606-621. <https://doi.org/10.1590/1678-4499.20180408>
- Xavier, A. C. F., Rudke, A. P., Fujita, T., Blain, G. C., Morais, M. V. B., Almeida, D. S., Rafee, S. A. A., Martins, L. D., Souza, R. A. F., Freitas, E. D. and Martins, J. A. (2019b). Stationary and non-stationary detection of extreme precipitation events and trends of average precipitation from 1980 to 2010 in the Paraná River basin, Brazil. *International Journal of Climatology*, 40:2, 1197-1212. <https://doi.org/10.1002/joc.6265>